ACS APPLIED MATERIALS & INTERFACES

Research Article

www.acsami.org

Micropatterned Surfaces for Atmospheric Water Condensation via Controlled Radical Polymerization and Thin Film Dewetting

Ian Wong,[†] Guo Hui Teo,[†,‡] Chiara Neto,[§] and Stuart C. Thickett*[,†,‡]

[†]Centre for Advanced Macromolecular Design (CAMD), School of Chemical Engineering, University of New South Wales, Sydney, New South Wales 2052, Australia

[‡]School of Physical Sciences (Chemistry), The University of Tasmania, Sandy Bay, Tasmania 7005, Australia

[§]School of Chemistry F11, The University of Sydney, Sydney, New South Wales 2006, Australia

Supporting Information

ABSTRACT: Inspired by an example found in nature, the design of patterned surfaces with chemical and topographical contrast for the collection of water from the atmosphere has been of intense interest in recent years. Herein we report the synthesis of such materials via a combination of macromolecular design and polymer thin film dewetting to yield surfaces consisting of raised hydrophilic bumps on a hydrophobic background. RAFT polymerization was used to synthesize poly(2-hydroxypropyl methacrylate) (PHPMA) of targeted molecular weight and low dispersity; spin-coating of PHPMA onto polystyrene films produced stable polymer bilayers under appropriate conditions. Thermal annealing of these bilayers above the glass transition temperature of the PHPMA layer led to complete dewetting of the top layer and the formation of isolated PHPMA domains atop the PS film. Due to the vastly different rates of water nucleation on the two phases, preferential dropwise nucleation of water occurred on the PHPMA domains, as demonstrated by optical microscopy. The simplicity of the preparation method and ability to target polymers of specific molecular weight demonstrate the value of these materials with respect to large-scale water collection devices or other materials science applications where patterning is required.

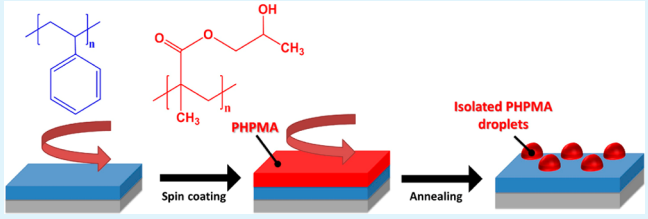

KEYWORDS: *dewetting, water collection, biomimicry, controlled radical polymerization, poly(hydroxypropyl methacrylate), wettability*

INTRODUCTION

Due to the pressing global challenge of water scarcity, alternative methods of water collection have become increasingly popular in recent years. One such example is the idea of atmospheric water-harvesting, whereby drinking water is collected via condensation onto a surface followed by subsequent collection and treatment.[1] This idea has been most impressively implemented by *FogQuest* for water collection within rural communities in Africa and South and Central America; the use of a high surface area polymer mesh results in the collection of over 200 L of water per day.[2] The simple, inexpensive, and sustainable nature of this approach is highly desirable in comparison to more energy-intensive methods of water purification and distribution.

One of the most popular examples of atmospheric water collection comes from the exceptional ability of *Stenocara dentata,* a member of the tenebrionidae family that lives in southwest Africa. *Stenocara* is able to survive in one of the driest climates on Earth[3] through the collection of drinking water via condensation on its patterned exoskeleton, achieved by flying into reliable fog-laden winds. The exoskeleton of *Stenocara* possesses chemical and topographical contrast, consisting of raised hydrophilic bumps (~0.5 mm diameter, 0.5−1.5 mm apart) on a waxy, hydrophobic background.[4] It is this surface structure that enables rapid dropwise nucleation and "pinning" on hydrophilic domains[5,6] when there is an appropriate temperature differential between the surface and surrounding air, effective droplet detachment to facilitate easy water collection, as well as minimizing loss through evaporation.[7,8]

After the elucidation of the water-harvesting mechanism of *Stenocara*, numerous attempts have been made to create synthetic surfaces that perform in an analogous manner. Such methods to prepare planar substrates have included the following: the manual deposition of polyelectrolytes onto a superhydrophobic substrate,[9] plasma-chemical treatment and deposition of various polymers using photomasks onto perfluorinated substrates,[8] UV photolithography[7] (including roll-type lithography[10]), laser-etching and computer-aided design,[11] chemical vapor deposition,[12] and inkjet printing.[13] One-dimensional water-harvesting fibers[14,15] and three-dimensional water-collecting devices[16] have also been reported (albeit based on different biomimetic design). This array of differing approaches is, however, often dependent on the need to first prepare a superhydrophobic substrate, in addition to using a synthetic approach that is not easy to scale up. Furthermore,

Received: July 27, 2015
Accepted: September 15, 2015
Published: September 15, 2015

DOI: 10.1021/acsami.5b06856
ACS Appl. Mater. Interfaces 2015, 7, 21562−21570

Table 1. Details of RAFT-Mediated Polymerization of HPMA, Molecular Weight Data, and Thermal Characteristics of the Samples

sample	target DP[a]	conversion[b]	expected DP	actual DP (^{1}H NMR)	M_n (^{1}H NMR) (kDa)	M_n (SEC) (kDa)	$Đ$	T_g (°C)	T_{10}/T_{50} (°C)[c]
PHPMA-1	96	0.43	41	33	5.1	9.6	1.22	87	204/333
PHPMA-2	291	0.26	76	75	11.1	18.0	1.11	85	206/345
PHPMA-3	402	0.85	342	n/a[d]	n/a	80.2	1.31	103	258/353

[a]As determined by the [HPMA]:[CPADB] ratio. [b]Calculated from ^{1}H NMR spectra taken immediately after polymerization. [c]Defined as temperature to reach 10% and 50% mass loss, respectively. [d]The signal from the dithiobenzoate end-group was not detected due to the high molecular weight of the sample.

several of these techniques are not suitable to pattern nonplanar substrates.

An additional approach to creating patterned water-collecting surfaces that was reported previously by our group is the spontaneous dewetting of polymer bilayer thin films.[17] Dewetting is a symmetry breaking process whereby an unstable liquid film transforms into its equilibrium states of a series of isolated droplets. Thin film (<100 nm) instability is due to unfavorable intermolecular forces between the film and the underlying substrate,[18−25] resulting in rupture, typically via heterogeneous nucleation and the formation of uncorrelated holes that grow with time and ultimately coalesce.[19,24,26−29] In the case of a thin polymer film, this mechanism occurs only when the system is annealed above the glass transition temperature (T_g) to enable sufficient mobility of the polymer melt; below T_g the dewetting pattern is essentially frozen in place. In our prior work, we created patterns from the spontaneous dewetting of hydrophilic poly(4-vinylpyridine) (P4VP) from hydrophobic polystyrene (PS) to yield surfaces with chemical and topographical contrast; this work represents an example of polymer bilayer dewetting where the top layer dewets from a metastable, but intact, bottom layer.[30−34] Such surfaces were shown to be effective at promoting water nucleation via dropwise condensation, resulting in a greater condensation rate than that of corresponding flat films, as well as facilitating water droplet detachment when tilted.[17] One of the significant advantages of this approach, with respect to other micropatterning methodologies, is the simplicity and scalability of the technique.

The requirements for a suitable hydrophilic polymer for a dewetted bilayer system described above include high T_g (well above room temperature) to prevent spontaneous dewetting, strong wettability contrast and immiscibility with the underlayer, negative spreading parameter, in addition to water insolubility. To that end, candidate polymers include (cross-linked) poly(*N*-vinylpyrrolidone),[35] poly(4-hydroxystyrene),[36,37] poly(4-vinylpyridine)[17,38] and various hydroxy-functional methacrylates.[39] Poly(2-hydroxypropyl methacrylate) (PHPMA) is one of the most suitable polymers to satisfy these criteria, with T_g ∼84 °C, static contact angle ∼70°,[39] and immiscibility with PS, and is predicted to dewet (i.e., the spreading parameter $S < 0$). It is also the lowest molecular weight poly(hydroxymethacrylate) that is water-insoluble [the more hydrophilic poly(2-hydroxyethyl methacrylate) is water-soluble below ∼2.5 kDa[40] and is softened and swollen with water at higher molecular weights]. PHPMA has been widely studied in recent times due to its utilization in all-aqueous dispersion polymerization systems[41] (the monomer, 2-hydroxypropyl methacrylate is water-soluble up to 13% w/w[42]) and polymerization-induced self-assembly;[43] however it has never been studied with respect to thin film dewetting and surface patterning.

With respect to polymer thin film dewetting, dewetting dynamics and mechanism are strongly influenced by the molecular weight of the polymer. The velocity of the dewetting front is inversely proportional to the melt viscosity of the polymer,[44] which in turn has a power-law dependence on molecular weight.[45−47] The density of nucleation in thin film dewetting is also higher in higher molecular weight polymers than in lower molecular weight polymers of the same composition, because the spin-coating of thin films induces a higher degree of internal stress in the films of very long chain polymers than in shorter chain polymers.[19] The higher nucleation density in turns leads to denser and smaller dewetted polymer droplets. The ability to systematically control polymer molecular weight is a feature of controlled/living radical polymerization (CLRP) techniques such as reversible addition−fragmentation chain transfer (RAFT) polymerization,[48,49] atom transfer radical polymerization[50] (ATRP), and nitroxide-mediated polymerization (NMP),[51] whereby a specific polymer chain length can be targeted through the molar ratio of monomer to control agent. RAFT polymerization is usually considered the most flexible of the controlled radical polymerization approaches, with excellent control of molecular weight at moderate reaction temperatures for a wide range of monomers. RAFT polymerization of HPMA has also been described recently through the use of dithiobenzoates to afford molecular weight control;[43,52,53] control of HPMA polymerization is important in this context as it is known to cross-link at high conversion and long chain lengths.[41]

In this work we report the preparation of micropatterned surface coatings consisting of PHPMA droplets on a PS background for evaluation and use as water-collecting surfaces. This is, to our knowledge, the first report of the dewetting of PHPMA from a nonwetting substrate. The ability to control macromolecular architecture is also considered by using RAFT polymerization to examine the effect of polymer molecular weight on the patterning process. The influence of molecular weight on dewetting dynamics and resultant surface morphology is demonstrated, as well as the performance of these surfaces with respect to heterogeneous nucleation of water droplets via condensation from humidified air. This biomimetic approach provides further insight into the ability to construct water-collecting devices in a facile manner.

EXPERIMENTAL SECTION

Materials. All chemicals listed were used as received except where otherwise stated. 2-Hydroxypropyl methacrylate (HPMA, 97%, consisting of a 75:25 mol:mol mixture of 2-hydroxypropyl and 2-hydroxyisopropyl isomers, Sigma-Aldrich) was deinhibited via passing through a basic aluminum oxide column (Ajax Finechem) and stored at 0 °C prior to use. 4-Cyanopentanoic acid dithiobenzoate (CPADB, >97%, Sigma-Aldrich) and 4,4′-azobis(4-cyanovaleric acid) (ACVA, >96%, Sigma-Aldrich) were stored in a refrigerator until use. Polystyrene (PS, M_p, 100 000 g mol^{-1}; M_w, 96 000 g mol^{-1}; M_n,

DOI: 10.1021/acsami.5b06856
ACS Appl. Mater. Interfaces 2015, 7, 21562−21570

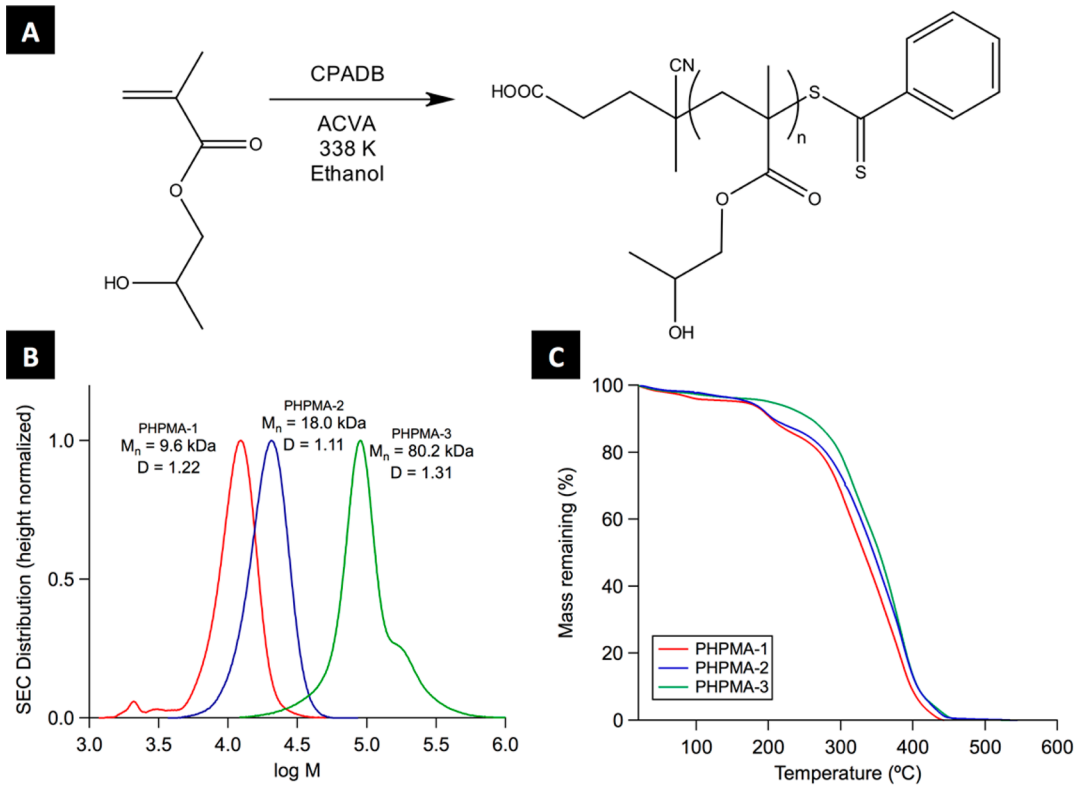

Figure 1. (A) RAFT-mediated polymerization of 2-hydroxypropyl methacrylate (HPMA); (B) SEC distributions of the three PHPMA samples described in Table 1; (C) thermogravimetric profiles of the three PHPMA samples.

92 000 g mol^{-1}; $Đ$, 1.04) standard PSS-PS100k sample was purchased from Polymer Standards Services. Solvents used in this work (anhydrous ethanol, diethyl ether) were purchased from Sigma-Aldrich and Chem Supply, respectively. The 1.0 × 1.0 cm^2 silicon wafers were prepared through diamond cutting of a larger polished, prime grade silicon wafer supplied by MMRC Pty Ltd., Australia.

RAFT Polymerization of HPMA. The general procedure used to prepare PHPMA of targeted molecular weight was as follows: deinhibited HPMA (2.55 g), ACVA, and CPADB were added to a round-bottom flask, in addition to 5 g of anhydrous ethanol. Three different PHPMA molecular weights were targeted (see Table 1) by adjusting the [HPMA]:[CPADB] ratio. The [CPADB]:[ACVA] ratio was held constant at 5. The round-bottom flask was sealed with a rubber septum, placed in an ice bath, and deoxygenated via bubbling with N_2 gas for 15 min. The solution was then transferred to an oil bath with thermostat set to 65 °C, and polymerization was conducted under constant magnetic stirring (400 rpm). Polymerization was ceased after a desired reaction time via quenching the reaction in an ice bath and opening the flask to air. Fractional conversion of monomer to polymer was determined via ^{1}H NMR spectroscopy in CD_3OD (see Polymer Characterization). The polymer samples were concentrated via partial removal of ethanol, and the polymer was precipitated via dropwise addition into diethyl ether. The precipitated solids were filtered, dried in a vacuum oven at 40 °C overnight, and stored in a desiccator until further use.

Polymer Characterization. PHPMA samples were characterized using a 300 MHz Bruker Avance III NMR spectrometer using CD_3OD as solvent. The internal solvent signal of CD_3OD was utilized for reference (δ = 3.31 ppm). Fractional conversion of monomer to polymer was calculated by considering the integral of the vinylic protons of the monomer (δ = 5.54−5.68 ppm and 6.05−6.17 ppm (set to 1)) with respect to the integration of the signal from δ = 3.73−4.18 ppm, attributed to the $-OCH_2-$ group of both the monomer and polymer.[54] ^{1}H NMR spectra of PHPMA were used to determine number-average degree of polymerization where possible by considering the integrals corresponding to the dithiobenzoate end group (δ = 7.35−7.93 ppm) and the $-OCH_2-$ present in each polymer repeat unit (δ = 3.73−4.18 ppm). Further details are provided in the Supporting Information.

Size exclusion chromatography (SEC) was performed on a Shimadzu system with four styragel columns (Polymer Labsoratories, 50, 100, 1000, and 10 000 nm pore sizes, plus guard column) in *N*,*N*-dimethylacetamide (DMAc) operating at a flow rate of 1 mL min^{-1} at 40 °C using a RID-10A refractive index detector. Chromatograms were analyzed by Cirrus SEC software version 3.0. The system was calibrated with a series of narrow molecular weight distribution polystyrene standards with molecular weights ranging from 0.5 to 1000 kDa.

Differential scanning calorimetry (DSC) analyses were performed using a PerkinElmer STA 6000 differential scanning calorimeter to determine the glass transition temperature (T_g) of the PHPMA samples. Three heating and cooling curves between 25 and 300 °C at a heating rate of 20 °C min^{-1} were collected for each sample.

Thermogravimetric analysis (TGA) was performed using a TGA Q5000 instrument (Polyscience, V3.15, Build 263) to determine the thermal decomposition profile of the PHPMA samples from 25 to 800 °C. TGA analyses were performed in a nitrogen environment, and data was collected using a heating rate of 10 °C min^{-1}.

Preparation of Polymer Monolayers and Bilayers via Spin-Coating. Cut Si wafers were cleaned via a multistep protocol prior to spin-coating as follows:[23] wafers were first sequentially sonicated for 1 min in distilled ethanol and distilled acetone and blow-dried with high purity nitrogen between each immersion. Wafers were then treated with a CO_2 snow jet to remove further contaminants, followed by 1 min of plasma treatment in a plasma cleaner (PDC-001, Harrick Plasma) to fully remove adsorbed contaminants on the Si surface. Solutions of PS in anhydrous toluene and PHPMA in anhydrous ethanol were prepared at concentrations of 20 mg mL^{-1} and 10 mg mL^{-1}, respectively, and subsequently filtered through a 0.45 μm nylon filter. Polymer monolayers and were prepared via spin-coating of these solutions (30 μL dispensed volume) for 1 min at 3000 rpm (Laurell Technologies WS 400B-6NPP/Lite spin coater); PS/PHPMA bilayers

DOI: 10.1021/acsami.5b06856
ACS Appl. Mater. Interfaces 2015, 7, 21562−21570

were prepared by sequential spin-coating of PS and then PHPMA using the same conditions described. Cleaning and spin-coating were performed in a laminar flow cabinet.

Polymer Thin Film Dewetting. The dewetting PHPMA/PS bilayers was conducted via thermal annealing using a TR-124 hot plate (ATV Technologies, Munich) at temperatures greater than 130 °C (above the bulk T_g values of both PS and PHPMA) in air. In some cases, dewetting was monitored using real-time optical microscopy (Nikon Eclipse LV150 optical microscope). After thermal annealing, the dewetted substrates were cooled to room temperature.

Thin Film Characterization. Static and dynamic water contact angle measurements were performed using a KSV CAM200 contact angle goniometer. Static contact angle measurements were performed by dispensing a 3 μL droplet (Milli-Q grade water) onto the substrate. Advancing contact angles were determined via the addition of a further 5 μL into the initial 3 μL droplet at an addition rate of 0.2 μL min^{-1}; the receding contact angle was determined using an analogous procedure.

The thicknesses of polymer monolayers and bilayers were determined via ellipsometry using a J.A. Woollam Co. spectroscopic ellipsometer (Model 2000 V) at an incident angle of 75°. Thickness measurements were taken across at least five points per substrate.

As-prepared and dewetted polymeric surfaces were analyzed via atomic force microscopy (AFM) using a Bruker Dimension Icon AFM in ScanAsyst mode. The scan rate in all cases was 1 Hz. AFM tips were triangular SCANASYST-AIR tips with a minimal force constant of 0.4 N m^{-1}. Images were typically collected over an area of 30 μm × 30 μm.

Evaluation of Atmospheric Water Collection. Evaluation of atmospheric condensation was performed using a custom-built apparatus attached to an optical microscope (Nikon LV150 optical microscope). A temperature-controlled Peltier plate encased in a humidified chamber with air supply was placed under the viewing stage of the microscope; the cooling stage was operated at 10 °C giving a temperature differential between the stage and surrounding air of ΔT = 10 °C. The flow of humidified air (RH ∼ 55%) or dry nitrogen across the surface could be alternated. Time-lapse optical microscopy of flat and dewetted surfaces upon exposure to cool humid air was performed to monitor water nucleation and condensation behavior. A photograph of the setup is provided in the Supporting Information.

RESULTS AND DISCUSSION

Synthesis and Characterization of PHPMA by RAFT Polymerization. In order to investigate the influence of polymer molecular weight on the suitability of PHPMA as a hydrophilic polymer in surface patterning applications, three different PHPMA samples were prepared via RAFT polymerization using CPADB to mediate the process (Figure 1A). The three PHPMA samples were designed to span close to an order of magnitude in number-average molecular weight (M_n). The dynamics of the dewetting process (in addition to resultant surface morphologies) is related to the melt viscosity of a polymer, which in turn has a power-law relationship ($\eta \propto M^{3.5}$) with respect to molecular weight.[45−47] As a result, an experimental study of the performance of these surfaces as a function of PHPMA molecular weight is paramount.

Information related to the polymerization process, polymer molecular weight, and thermal properties of the polymers produced is presented in Table 1. In the case of PHPMA-1 and PHPMA-2, the relatively low expected degree of polymerization (41 and 76, respectively) enabled determination of the number-average DP (and hence M_n) by end group analysis via ^{1}H NMR spectroscopy. This was not possible in the case of sample PHPMA-3, where the signal from the dithiobenzoate end group was not detectable by ^{1}H NMR due to the much higher number of HPMA repeat units. SEC analysis (see Figure 1B) revealed polymers with low dispersity values and molecular weight distributions that were monomodal in nature, with the exception of PHPMA-3; the high molecular weight shoulder observed in this case was attributed to the formation of dead polymer chains via combination, a phenomenon seen at high conversion of monomer to polymer.[55] The dispersity value for the high molecular weight PHPMA-3 reported here is significantly lower than previously reported RAFT solution polymerization of HPMA where a high DP was targeted.[41] M_n values determined by SEC are consistently higher than those predicted from experiment (by a factor of approximately 1.6), a difference that is expected given that the SEC is calibrated with respect to linear polystyrene standards. Despite these molecular weight averages being relative, the expected trend of increasing molecular weight is clear. The glass transition temperatures (T_g) of the three samples were comparable to previously reported values for PHPMA;[56] TGA analysis revealed increasing thermal stability with polymer molecular weight (Figure 1C), with all samples essentially thermally stable in the temperature range required for thin film dewetting (<10% mass loss at 200 °C in all cases, see T_{10} values in Table 1).

Wettability and Surface Morphology of PHPMA Films. The three PHPMA samples described above were subsequently used to prepare PHPMA thin films via spin-coating from dilute ethanol solution (10 mg mL^{-1}), using cleaned Si wafers as substrate. The average film thickness as measured by ellipsometry was nearly identical for the three different samples at 34.4 (±0.2 nm), and the refractive index for PHPMA was estimated to be ∼1.502 ± 0.004, which was in good agreement with the published value of 1.512.[57]

Surface roughness and wettability for the three PHPMA films were studied by atomic force microscopy (AFM) in addition to both static and dynamic contact angle measurements, the results of which are presented in Table 2 and Figure 2. In comparison to PS films prepared by spin-coating, where the root-mean-square (RMS) roughness is typically very low (0.16 ± 0.05 nm in experiments performed in this work), the roughness of our PHPMA monolayers was significantly higher (always >1 nm; see Table 2). Inspection of the AFM topography images for the three different PHPMA samples shows that the films possess a certain degree of ordered surface texture or correlated microstructure, particularly in the case of PHPMA-3, somewhat analogous to phase separated block copolymer films. The periodicity of the features in these images increases with increasing molecular weight (based on 2D FFT analysis of the images in Figure 2), from 0.66 μm for PHPMA-1 to 1.29 μm for PHPMA-2 to 1.75 μm for PHPMA-3. The origin of this increased surface roughness and microstructuring in these systems is not fully understood, given the high solubility of PHPMA in ethanol (>30% w/w during polymer synthesis). Surface microstructuring was not observed in bilayer PHPMA/PS systems, suggesting an influence due to the Si substrate. One possible cause may be the partial trapping of

Table 2. RMS Roughness Values and Contact Angle Measurements for PS and PHPMA Surfaces Used in This Work

sample	RMS roughness (nm)	θ_{eq} (deg)	θ_{adv} (deg)	θ_{rec} (deg)
PS	0.16 ± 0.05	89 ± 1	96 ± 2	73 ± 1
PHPMA-1	1.5 ± 0.07	44 ± 3	55 ± 3	<5
PHPMA-2	2.8 ± 0.15	56 ± 1	69 ± 2	<5
PHPMA-3	0.99 ± 0.06	57 ± 2	85 ± 2	17 ± 2

DOI: 10.1021/acsami.5b06856
ACS Appl. Mater. Interfaces 2015, 7, 21562−21570

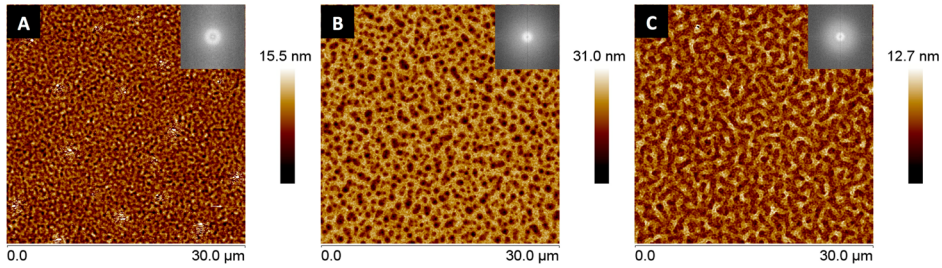

Figure 2. AFM topography images of (A) PHPMA-1, (B) PHPMA-2, (C) PHPMA-3 monolayer films prepared on Si. Inset: 2D FFT analyses of the surface topography.

solvent (ethanol) during the spin-coating process, which would be stronger on the Si substrate than on the PS bottom layer. Alternatively, the inclusion of water through atmospheric humidity during and after surface preparation is also expected to be higher on a hydrophilic Si substrate than on the hydrophobic PS. Inclusion of water during the spin-coating process will affect both the solvent contact angle and evaporation rate, which are both known to contribute to surface roughness.[58] A partial swelling of the polymer can also not be discounted, given the water solubility of the HPMA monomer.

Static and dynamic contact angle measurements for PHPMA films revealed a strong dependence on polymer molecular weight. The lowest molecular weight sample (PHPMA-1) had a much lower static and advancing contact angle than the other two substrates (lower than the equilibrium contact angle of PHPMA-2 and PHPMA-3); the static contact angle decreased initially from ∼50° to its equilibrium value, and no receding contact angle was measurable. Indeed, the only substrate where a receding contact angle was successfully measured was PHPMA-3 (17°), a surface that possessed an extremely large contact angle hysteresis (68°). We rationalize this behavior on the basis of (partial) water solubility of PHPMA chains at relatively low average chain lengths. As highlighted in the Introduction, HPMA is a water-soluble monomer (up to a concentration of 13% w/w), but its polymer is water-insoluble. Given the success in implementing HPMA in all-aqueous dispersion polymerization systems,[52,53] a growing PHPMA chain will continually decrease with respect to water solubility until it can be considered water-insoluble. Given the relatively low average degree of polymerization for samples PHPMA-1 and PHPMA-2, it is plausible that these samples are partially dissolving, or at least swelling, when in contact with water. This was supported by a simple water immersion experiment where, after 30 min in deionized water, the PHPMA-1 film had completely delaminated, and the PHPMA-2 surface had become cracked in various places (see Supporting Information). Conversely, films of PHPMA-3 demonstrated excellent stability with respect to water with no change in measured contact angle and only a 3% decrease in film thickness.

PHPMA/PS Bilayer Preparation and Thin Film Dewetting. PHPMA/PS bilayers were prepared via sequential spin-coating of PS (from toluene) and PHPMA (from ethanol) using the three differing PHPMA samples as detailed above. In all cases the preparation conditions for the PS underlayer were identical, with an average layer thickness of 74.4 ± 0.1 nm as determined by ellipsometry. The thickness of the top PHPMA layer was measured to be ∼35 nm in all cases; despite ellipsometry data suggesting a uniform polymer bilayer in the case of PHPMA-1/PS, this was in fact not the case and is discussed below. The two highest molecular weight PHPMA samples (PHPMA-2 and PHPMA-3) yielded stable polymer bilayers following their preparation; however, the PHPMA-1/PS bilayer exhibited spontaneous partial dewetting at room temperature in the absence of any additional stimuli, known as spin dewetting[59,60] (Figure 3). Given the relatively low degree

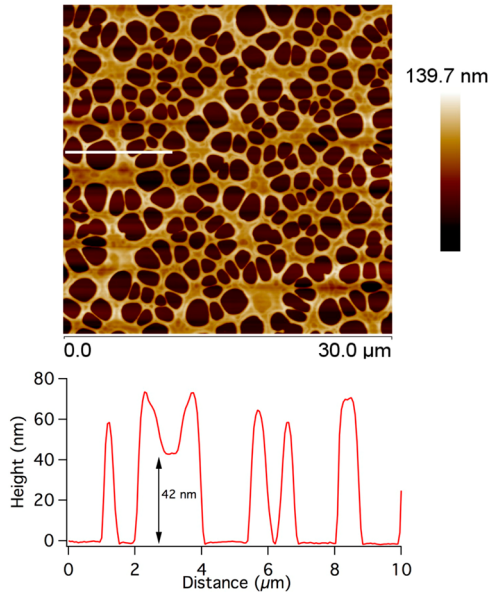

Figure 3. AFM topography image (upper panel) of PHPMA-1/PS bilayer after spontaneous dewetting of the uppermost PHPMA layer following sample preparation. Lower panel shows AFM topography line profile of region indicated.

of polymerization of PHPMA-1 (∼33 HPMA units per chain), we postulate that the T_g of the thin PHPMA-1 film system is below room temperature, as previously observed for polymer films of thickness smaller than 100 nm,[61] which would enable the PHPMA-1 layer to be significantly more dynamic than the other samples considered. Due to the combination of high water solubility and the inability to prepare stable bilayers, PHPMA-1 was not examined further with respect to micropatterned surface preparation.

The PHPMA-2/PS and PHPMA-3/PS bilayers were studied with respect to dewetting dynamics upon thermal annealing above the glass transition temperature. PHPMA is predicted to dewet from PS due to the spreading parameter $S < 0$ (see Supporting Information); however, this is the first experimental demonstration of this phenomenon. It is additionally worth noting that the spreading parameter of PS on Si/SiO*x* is small but negative ($S \sim -0.26$ mN m^{-1}),[62] and the PS underlayer is

DOI: 10.1021/acsami.5b06856
ACS Appl. Mater. Interfaces 2015, 7, 21562−21570

metastable on this substrate, but no dewetting of PS was observed. Despite the bulk T_g of both PHPMA samples measured as 85 and 103 °C, respectively, dewetting was not observed to occur until an annealing temperature of 130 °C in both systems. A similar delay in the onset of dewetting has been observed previously by our group for poly(4-vinylpyridine)[62] as well as for poly(lactide-*co*-glycolide)[63] on PS substrates, which we attribute to viscous dissipation at the interface between the two layers. At 130 °C dewetting proceeds via heterogeneous nucleation through the formation of uncorrelated holes that increase in size with annealing time (see Supporting Information). The growth of dewetted holes prior to coalescence was strongly nonlinear in both cases, indicating viscous forces and interfacial slip at the PHPMA/PS boundary.[64,65] There is a significantly greater density of nucleated holes in the PHPMA-3/PS system (~8100 per mm^2) compared to the lower molecular weight PHPMA-2/PS system (~130 per mm^2), an observation that is in agreement with previous work considering the influence of polymer molecular weight on dewetting.[19] With a view toward the preparation of micropatterned surfaces that mimic *Stenocara*, elevating the annealing temperature to 150 °C resulted in rapid and complete dewetting in both systems (see Figure 4),

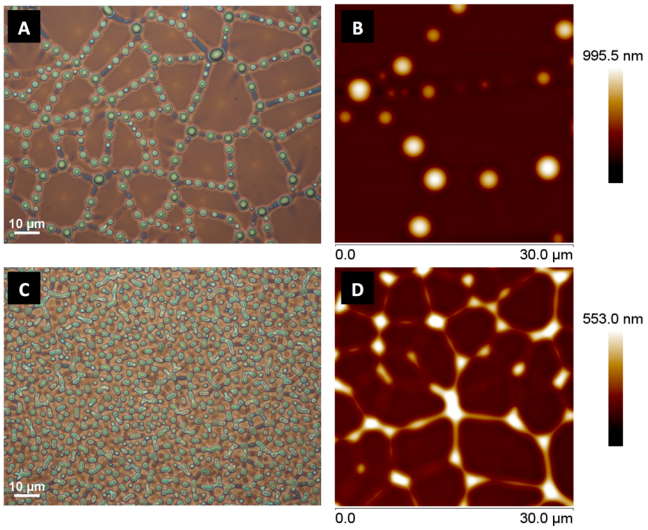

Figure 4. Optical microscopy and AFM topography images of fully dewetted PHPMA/PS bilayers: (A and B) PHPMA-2/PS; (C and D) PHPMA-3/PS.

resulting in surfaces that consisted either of isolated droplets or a series of droplets and interconnected cylinders. Topographical analysis of these surfaces via AFM indicated that the PHPMA domains were between 0.3 and 1.0 μm in height for PHPMA-2 and 0.1 and 0.5 μm for PHPMA-3, with a significantly greater hydrophilic domain density in the case of PHPMA-3 (9.4 (±0.5) × 10^3 mm^{-2}) compared to PHPMA-2 (2.4 (±0.2) × 10^3 mm^{-2}). Topographical analysis also demonstrated slight deformation of the PS underlayer, indicative of a liquid−liquid dewetting regime.[30] Given the structure of these films with respect to hydrophilic domains on a hydrophobic background, they represent mimics of the *Stenocara* exoskeleton on a different scale.[4]

Evaluation of Atmospheric Water Condensation. Prior to the analysis of condensation on micropatterned surfaces, condensation on flat PS and PHPMA films (PHPMA-2 and PHPMA-3) was observed via optical microscopy, using a cooling stage set ~10 °C below the ambient air temperature (RH ~ 55%). Water droplets immediately begin to nucleate on both surfaces (see Figure 5), with vastly different droplet

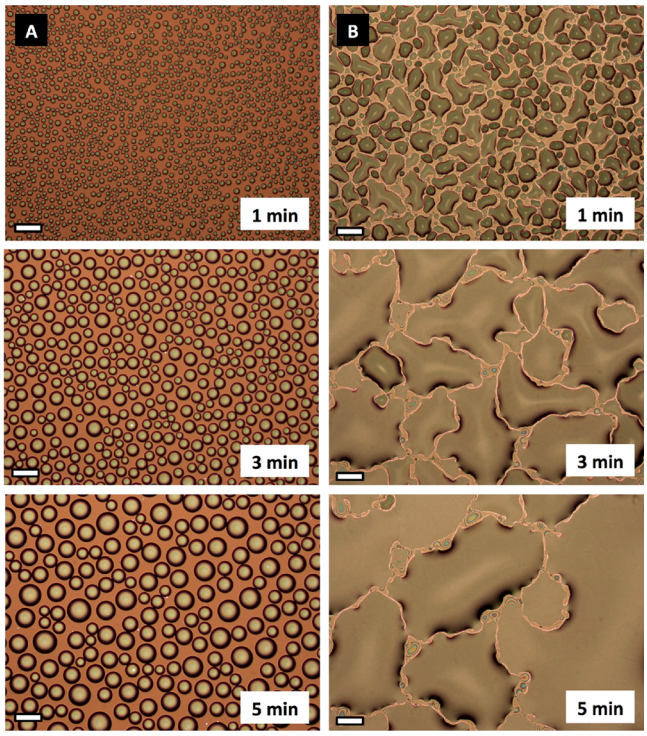

Figure 5. Optical microscopy images demonstrating the appearance of condensed water droplets on (A) PS and (B) PHPMA surfaces upon exposure to humid air (55% RH) over a 5 min period. The scale bar in all cases is 50 μm.

morphologies due to the different wettability of the two materials. Water droplets on the PS surface were highly rounded in nature, whereas on the PHPMA surfaces irregular and elongated water droplets quickly formed. After ~5 min, the PHPMA substrate was almost completely covered in a film of water due to coalescence of neighboring water droplets, leading to filmwise condensation, whereas discrete droplets still existed on the PS surface.

The large difference in the condensation pattern on flat PS and PHPMA substrates has significant implications with respect to the condensation of water on our micropatterned PHPMA/PS surfaces. Figure 6 shows the condensation pattern initially formed on a PHPMA-2/PS substrate upon exposure to humid air with a temperature differential between the substrate and surrounding air of 10 °C. Water droplets rapidly nucleate on the dewetted PHPMA domains, but not the PS background, and grow with time via coalescence with neighboring droplets. This nucleation mechanism is analogous to the nucleation mechanism reported for *Stenocara*[4] as well as that reported previously by our group for micropatterned substrates[17] prepared from commercially available polymer standards. This highly preferential heterogeneous nucleation of water on PHPMA domains is due to the difference in the free energy barrier ($\Delta\Delta G$) to condensation on hydrophilic surfaces compared to hydrophobic ones[5,66,67] based on the macroscopic contact angle; we estimate a difference in the nucleation rate between the two phases on the order of ~10.[46] At the same

DOI: 10.1021/acsami.5b06856
ACS Appl. Mater. Interfaces 2015, 7, 21562−21570

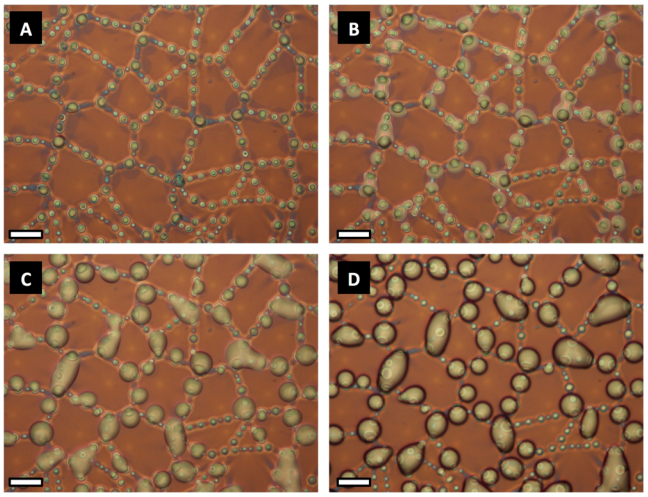

Figure 6. Optical microscopy images of condensed water droplets on a dewetted PHPMA-2/PS surface after (A) 1 s, (B) 20 s, (C) 100 s, and (D) 150 s exposure to humid air. The scale bar in all cases is 10 μm.

time, as the heat-transfer coefficient for dropwise condensation is much larger than that for filmwise condensation, it becomes important to prepare patterns that are mostly hydrophobic.[68]

The surface structuring generated by the dewetting process thus addresses both these issues, presenting a lower barrier to nucleation with its hydrophilic bumps, and a higher rate of cooling due to dropwise condensation. As a result of these effects, patterned surfaces by dewetting will collect more atmospheric water than flat surfaces of any wettability. As was the case for flat PHPMA-2 films, some swelling of the PHPMA-2 domains was observed on the dewetted substrates after condensation (see Supporting Information), a phenomenon not observed at the highest molecular weight studied.

Additionally, the creation of micropatterned polymer surfaces such as those reported here facilitates easier macroscopic water droplet detachment compared to featureless hydrophilic films. In comparison to flat PHPMA surfaces (see Table 2), the dewetted PHPMA-3/PS surface had a significantly reduced contact angle hysteresis (θ_{adv} = 95.0°, θ_{rec} = 54.2°). As droplet detachment is related to the contact angle hysteresis on a tilted substrate via the Furmidge equation,[69] we predict a reduction in the critical droplet volume V_{crit} (the smallest droplet of water that will successfully detach from a surface) from ~55 μL (on PHPMA) to ~23 μL (on the dewetted substrate). Given the size of the hydrophilic domains on these surfaces, a water droplet of this volume will be in contact with tens of thousands of PHPMA "bumps", which is mechanistically different from *Stenocara*. Nonetheless, the design of materials that promote dropwise condensation and enable facile droplet detachment aids in the continual collection of water from the atmosphere.

CONCLUSIONS

In the present work, we report the preparation of micropatterned surfaces with both chemical and topographical contrast via the combination of controlled/living radical polymerization and the dewetting of polymer thin films. Immiscible polymer bilayers of PHPMA on top of PS were prepared by sequential spin-coating; thermal annealing above the T_g produced a surface pattern consisting of isolated domains (droplets and/or droplets with interconnected cylinders) of hydrophilic PHPMA on a hydrophobic PS background. The strong wettability contrast between the two phases enabled these materials to serve as highly effective surfaces for the heterogeneous nucleation of water; upon cooling these surfaces to a temperature 10 K lower than the ambient air temperature, rapid nucleation and condensation of water took place solely on the PHPMA phase, followed by water droplet growth and coalescence. The ability for the PHPMA domains to act as seeding points for dropwise condensation is highly advantageous with respect to preparing water-collecting surfaces, as the contact angle hysteresis on these surfaces is significantly lower than their flat hydrophilic counterparts. As contact angle hysteresis governs droplet detachment from tilted substrates, these micropatterned substrates enable a greater frequency of nucleation, growth, and detachment cycles.

In addition to the applied context of these materials, this work also serves as the first demonstration of micropatterning via dewetting of PHPMA, in addition to the applicability of controlled/living radical polymerization (CLRP) in developing a greater understanding of polymer thin film dynamics. PHPMA is a polymer that has received increased interest in recent times due to its water-insolubility and applicability in polymer self-assembly, but has not previously been the focus of work as a thin film surface coating or in surface micropatterning. PHPMA readily dewets via heterogeneous nucleation from substrates such as PS due to unfavorable intermolecular forces at the bilayer interface; the dewetting process can be readily stopped by reducing the temperature below T_g. The marked influence of PHPMA molecular weight was highlighted through both the resultant micropattern at the end of the dewetting process, as well as the robustness of the materials toward water exposure. At very low molecular weights stable polymer bilayers could not be prepared, whereas at high molecular weights the films demonstrate no swelling or degradation. The convenience of designing polymers with targeted molecular weight and low dispersity through techniques such as RAFT polymerization, as shown here, allows for the features of a dewetted bilayer system to be readily tuned.

Given the ability for thin polymer films to be prepared on nonplanar substrates and across large surface areas, we believe that the approach outlined here is highly relevant for the creation of large-scale patterned materials. Such large-scale surfaces could be prepared by depositing polymers on substrates by techniques including dip coating or spraying. The size and density of patterned features on surfaces prepared by dewetting can also be adjusted through relatively simple modifications to the preparation technique, such as changing the film thickness or preannealing the film at a relatively low temperature. In addition to water-collecting substrates, these materials may also serve as an interesting platform in various biological applications where site-specific adhesion of biomolecules is desired on the basis of chemical and topographical contrast.

ASSOCIATED CONTENT

Supporting Information

The Supporting Information is available free of charge on the ACS Publications website at DOI: 10.1021/acsami.5b06856.

NMR spectra, spreading parameter calculations, contact angle measurements, AFM topography, and optical microscopy images (PDF)

DOI: 10.1021/acsami.5b06856
ACS Appl. Mater. Interfaces 2015, 7, 21562−21570

AUTHOR INFORMATION

Corresponding Author

*E-mail: stuart.thickett@utas.edu.au. Phone: +61-3-6226-2783. Fax: +61-3-6226-2758.

Author Contributions

Experimental work was conducted by I.W. and G.H.T. in the laboratories of C.N. and S.T. The manuscript was written through contributions of all authors. All authors have given approval to the final version of the manuscript.

Funding

Funding from the Australian Research Council Linkage Grants scheme (LP130100088) is gratefully acknowledged.

Notes

The authors declare no competing financial interest.

ACKNOWLEDGMENTS

S.C.T. acknowledges the University of New South Wales for the provision of a Vice-Chancellor's Post-Doctoral Research Fellowship. Omar Al-Khayat is acknowledged for designing the controlled-humidity cooling chamber.

REFERENCES

(1) Vince, G. Out of the Mist. *Science* **2010**, *330*, 750−751.
(2) *FogQuest*; http://www.fogquest.org (accessed Accessed April 21).
(3) Henschel, J. R.; Seely, M. K. Ecophysiology of Atmospheric Moisture in the Namib Desert. *Atmos. Res.* **2008**, *87*, 362−368.
(4) Parker, A. R.; Lawrence, C. R. Water Capture by a Desert Beetle. *Nature* **2001**, *414*, 33−34.
(5) Varanasi, K. K.; Hsu, M.; Bhate, N.; Yang, W.; Deng, T. Spatial Control in the Heterogeneous Nucleation of Water. *Appl. Phys. Lett.* **2009**, *95* (9), 094101−3.
(6) Varanasi, K. K.; Tao, D. In *Controlling Nucleation and Growth of Water using Hybrid Hydrophobic-Hydrophilic Surfaces*, 12th IEEE Intersociety Conference on Thermal and Thermomechanical Phenomena in Electronic Systems (ITherm), 2−5 June 2010; 2010; pp 1−5.
(7) Dorrer, C.; Ruehe, J. Mimicking the Stenocara Beetle - Dewetting of Drops From a Patterned Superhydrophobic Surface. *Langmuir* **2008**, *24*, 6154−6158.
(8) Garrod, R. P.; Harris, L. G.; Schofield, W. C. E.; McGettrick, J.; Ward, L. J.; Teare, D. O. H.; Badyal, J. P. S. Mimicking a Stenocara Beetle's Back for Microcondensation Using Plasmachemical Patterned Superhydrophobic-Superhydrophilic Surfaces. *Langmuir* **2007**, *23* (2), 689−693.
(9) Zhai, L.; Berg, M. C.; Cebeci, F. C.; Kim, Y.; Milwid, J. M.; Rubner, M. F.; Cohen, R. E. Patterned Superhydrophobic Surfaces; Toward a Synthetic Mimic of the Namib Desert Beetle. *Nano Lett.* **2006**, *6* (6), 1213−1217.
(10) Lee, S.; Lee, J.; Park, C.; Lee, C.; Kim, K.; Tahk, D.; Kwak, M. Continuous Fabrication of Bio-Inspired Water Collecting Surface via Roll-Type Photolithography. *Int. J. of Precis. Eng. and Manuf.-Green Technol.* **2014**, *1* (2), 119−124.
(11) Ghosh, A.; Beaini, S.; Zhang, B. J.; Ganguly, R.; Megaridis, C. M. Enhancing Dropwise Condensation through Bioinspired Wettability Patterning. *Langmuir* **2014**, *30* (43), 13103−13115.
(12) Kim, G.-T.; Gim, S.-J.; Cho, S.-M.; Koratkar, N.; Oh, I.-K. Wetting-Transparent Graphene Films for Hydrophobic Water-Harvesting Surfaces. *Adv. Mater.* **2014**, *26* (30), 5166−5172.
(13) Zhang, L.; Wu, J.; Hedhili, M. N.; Yang, X.; Wang, P. Inkjet Printing for Direct Micropatterning of a Superhydrophobic Surface: Toward Biomimetic Fog Harvesting Surfaces. *J. Mater. Chem. A* **2015**, *3* (6), 2844−2852.
(14) Chen, Y.; Zheng, Y. Bioinspired Micro-/Nanostructure Fibers with a Water Collecting Property. *Nanoscale* **2014**, *6* (14), 7703−7714.
(15) Hou, Y.; Gao, L.; Feng, S.; Chen, Y.; Xue, Y.; Jiang, L.; Zheng, Y. Temperature-Triggered Directional Motion of Tiny Water Droplets on Bioinspired fibers in Humidity. *Chem. Commun.* **2013**, *49* (46), 5253−5255.
(16) Cao, M.; Ju, J.; Li, K.; Dou, S.; Liu, K.; Jiang, L. Facile and Large-Scale Fabrication of a Cactus-Inspired Continuous Fog Collector. *Adv. Funct. Mater.* **2014**, *24* (21), 3235−3240.
(17) Thickett, S. C.; Neto, C.; Harris, A. T. Biomimetic Surface Coatings for Atmospheric Water Capture Prepared by Dewetting of Polymer Films. *Adv. Mater.* **2011**, *23*, 3718−3722.
(18) Reiter, G. Dewetting of Highly Elastic Thin Polymer Films. *Phys. Rev. Lett.* **2001**, *87*, 186101.
(19) Reiter, G.; Hamieh, M.; Damman, P.; Sclavons, S.; Gabriele, S.; Vilmin, T.; Raphael, E. Residual Stresses in Thin Polymer Films Cause Rupture and Dominate Early Stages of Dewetting. *Nat. Mater.* **2005**, *4*, 754−758.
(20) de Gennes, P. G. Wetting: Statics and Dynamics. *Rev. Mod. Phys.* **1985**, *57* (3), 827.
(21) Neto, C. A Novel Approach to the Micropatterning of Proteins Using Dewetting of Polymer Bilayers. *Phys. Chem. Chem. Phys.* **2007**, *9*, 149−155.
(22) Neto, C.; Jacobs, K. Dynamics of Hole Growth in Dewetting Polystyrene Films. *Phys. A* **2004**, *339* (1−2), 66−71.
(23) Neto, C.; Jacobs, K.; Seemann, R.; Blossey, R.; Becker, J.; Gruen, G. Satellite Hole Formation During Dewetting: Experiment and Simulation. *J. Phys.: Condens. Matter* **2003**, *15*, 3355−3366.
(24) Sharma, A.; Khanna, R. Pattern Formation in Unstable Thin Liquid Films. *Phys. Rev. Lett.* **1998**, *81* (16), 3463−3466.
(25) Xie, R.; Karim, A.; Douglas, J. F.; Han, C. C.; Weiss, R. A. Spinodal Dewetting of Thin Polymer Films. *Phys. Rev. Lett.* **1998**, *81* (6), 1251−1254.
(26) Blossey, R. Nucleation at First-Order Wetting Transitions. *Int. J. Mod. Phys. B* **1995**, *09* (27), 3489−3525.
(27) Stange, T. G.; Evans, D. F.; Hendrickson, W. A. Nucleation and Growth of Defects Leading to Dewetting of Thin Polymer Films. *Langmuir* **1997**, *13* (16), 4459−4465.
(28) Jacobs, K.; Herminghaus, S.; Mecke, K. R. Thin Liquid Polymer Films Rupture via Defects. *Langmuir* **1998**, *14* (4), 965−969.
(29) Reiter, G. Dewetting of Thin Polymer Films. *Phys. Rev. Lett.* **1992**, *68* (1), 75−78.
(30) Brochard-Wyart, F.; Martin, P.; Redon, C. Liquid/liquid Dewetting. *Langmuir* **1993**, *9* (12), 3682−3690.
(31) Krausch, G. Dewetting at the Interface Between Two Immiscible Polymers. *J. Phys.: Condens. Matter* **1997**, *9*, 7741−7752.
(32) Li, C.; Jiang, J.; Rafailovich, M. H.; Sokolov, J. Melt Fracture in Polymer Thin Films at Strongly Attractive Surfaces. *Europhys. Lett.* **2006**, *76* (5), 870−876.
(33) de Silva, J. P.; Geoghegan, M.; Higgins, A. M.; Krausch, G.; David, M. O.; Reiter, G. Switching Layer Stability in a Polymer Bilayer by Thickness Variation. *Phys. Rev. Lett.* **2007**, *98*, 267802.
(34) Paul, R.; Karabiyik, U.; Swift, M. C.; Hottle, J. R.; Esker, A. R. Morphological Evolution in Dewetting Polystyrene/Polyhedral Oligomeric Silsesquioxane Thin Film Bilayers. *Langmuir* **2008**, *24* (9), 4676−4684.
(35) Telford, A. M.; Thickett, S. C.; James, M.; Neto, C. Competition Between Dewetting and Cross-Linking in Poly(N-vinylpyrrolidone)/Polystyrene Bilayer Films. *Langmuir* **2011**, *27* (23), 14207−14217.
(36) Gesser, H. D.; Lafreniere, D. R. T. A Drag-Reducing Water Insoluble Hydrophilic Marine Coating. *Prog. Org. Coat.* **2004**, *49* (4), 372−374.
(37) Prolongo, M. G.; Salom, C.; Masegosa, R. M. Glass Transitions and Interactions in Polymer Blends Containing Poly(4-hydroxystyrene) Brominated. *Polymer* **2002**, *43* (1), 93−102.
(38) Shibata, M.; Kimura, Y.; Yaginuma, D. Thermal Properties of Novel Supramolecular Polymer Networks Based on Poly(4-vinylpyridine) and Disulfonic Acids. *Polymer* **2004**, *45* (22), 7571−7577.
(39) Kou, P. M.; Pallassana, N.; Bowden, R.; Cunningham, B.; Joy, A.; Kohn, J.; Babensee, J. E. Predicting Biomaterial Property-Dendritic Cell Phenotype Relationships From the Multivariate Analysis of

DOI: 10.1021/acsami.5b06856
ACS Appl. Mater. Interfaces 2015, 7, 21562−21570

Responses to Polymethacrylates. *Biomaterials* **2012**, *33* (6), 1699−1713.
(40) Paterson, S. M.; Brown, D. H.; Chirila, T. V.; Keen, I.; Whittaker, A. K.; Baker, M. V. The Synthesis of Water-Soluble PHEMA via ARGET ATRP in Protic Media. *J. Polym. Sci., Part A: Polym. Chem.* **2010**, *48* (18), 4084−4092.
(41) Ali, A. M. I.; Pareek, P.; Sewell, L.; Schmid, A.; Fujii, S.; Armes, S. P.; Shirley, I. M. Synthesis of Poly(2-hydroxypropyl methacrylate) Latex Particles via Aqueous Dispersion Polymerization. *Soft Matter* **2007**, *3* (8), 1003−1013.
(42) Madsen, J.; Armes, S. P.; Lewis, A. L. Preparation and Aqueous Solution Properties of New Thermoresponsive Biocompatible ABA Triblock Copolymer Gelators. *Macromolecules* **2006**, *39* (22), 7455−7457.
(43) Li, Y.; Armes, S. P. RAFT Synthesis of Sterically Stabilized Methacrylic Nanolatexes and Vesicles by Aqueous Dispersion Polymerization. *Angew. Chem., Int. Ed.* **2010**, *49* (24), 4042−4046.
(44) Wang, C.; Krausch, G.; Geoghegan, M. Dewetting at a Polymer−Polymer Interface: Film Thickness Dependence. *Langmuir* **2001**, *17* (20), 6269−6274.
(45) de Gennes, P. G. Reptation of a Polymer Chain in the Presence of Fixed Obstacles. *J. Chem. Phys.* **1971**, *55* (2), 572−579.
(46) Des Cloizeaux, J. Polymer Melt: Reptation of a Chain and Viscosity. *J. Phys., Lett.* **1984**, *45*, 17−26.
(47) Doi, M.; Edwards, S. F. Dynamics of Concentrated Polymer Systems. Part 1.-Brownian Motion in the Equilibrium State. *J. Chem. Soc., Faraday Trans. 2* **1978**, *74* (0), 1789−1801.
(48) Chiefari, J.; Chong, Y. K.; Ercole, F.; Krstina, J.; Jeffery, J.; Le, T. P. T.; Mayadunne, R. T. A.; Meijs, G. F.; Moad, C. L.; Moad, G.; Rizzardo, E.; Thang, S. H. Living Free-Radical Polymerization by Reversible Addition-Fragmentation Chain Transfer: The RAFT Process. *Macromolecules* **1998**, *31*, 5559−5562.
(49) Moad, G.; Chong, Y. K.; Postma, A.; Rizzardo, E.; Thang, S. H. Advances in RAFT Polymerization: The Synthesis of Polymers With Defined End-Groups. *Polymer* **2005**, *46*, 8458−8468.
(50) Matyjaszewski, K.; Tsarevsky, N. V. Macromolecular Engineering by Atom Transfer Radical Polymerization. *J. Am. Chem. Soc.* **2014**, *136* (18), 6513−6533.
(51) Nicolas, J.; Guillaneuf, Y.; Lefay, C.; Bertin, D.; Gigmes, D.; Charleux, B. Nitroxide-Mediated Polymerization. *Prog. Polym. Sci.* **2013**, *38* (1), 63−235.
(52) Sugihara, S.; Armes, S. P.; Blanazs, A.; Lewis, A. L. Non-Spherical Morphologies from Cross-Linked Biomimetic Diblock Copolymers using RAFT Aqueous Dispersion Polymerization. *Soft Matter* **2011**, *7* (22), 10787−10793.
(53) Sugihara, S.; Blanazs, A.; Armes, S. P.; Ryan, A. J.; Lewis, A. L. Aqueous Dispersion Polymerization: A New Paradigm for in Situ Block Copolymer Self-Assembly in Concentrated Solution. *J. Am. Chem. Soc.* **2011**, *133* (39), 15707−15713.
(54) Zehm, D.; Ratcliffe, L. P. D.; Armes, S. P. Synthesis of Diblock Copolymer Nanoparticles via RAFT Alcoholic Dispersion Polymerization: Effect of Block Copolymer Composition, Molecular Weight, Copolymer Concentration, and Solvent Type on the Final Particle Morphology. *Macromolecules* **2013**, *46* (1), 128−139.
(55) Moad, G.; Rizzardo, E.; Thang, S. H. Radical Addition−Fragmentation Chemistry in Polymer Synthesis. *Polymer* **2008**, *49* (5), 1079−1131.
(56) Dai, J.; Goh, S. H.; Lee, S. Y.; Slow, K. S. Complexation Between Poly(2-hydroxypropyl methacrylate) and Three Tertiary Amide Polymers. *J. Appl. Polym. Sci.* **1994**, *53* (7), 837−845.
(57) Brandrup, J.; Immergut, E. H. *Polymer Handbook*, 3rd ed.; John Wiley and Sons, Inc.: New York, 1989.
(58) Strawhecker, K. E.; Kumar, S. K.; Douglas, J. F.; Karim, A. The Critical Role of Solvent Evaporation on the Roughness of Spin-Cast Polymer Films. *Macromolecules* **2001**, *34* (14), 4669−4672.
(59) Bhandaru, N.; Das, A.; Salunke, N.; Mukherjee, R. Ordered Alternating Binary Polymer Nanodroplet Array by Sequential Spin Dewetting. *Nano Lett.* **2014**, *14* (12), 7009−7016.
(60) Ferrell, N.; Hansford, D. Fabrication of Micro- and Nanoscale Polymer Structures by Soft Lithography and Spin Dewetting. *Macromol. Rapid Commun.* **2007**, *28* (8), 966−971.
(61) Herminghaus, S.; Jacobs, K.; Seemann, R. Viscoelastic Dynamics of Polymer Thin Films and Surfaces. *Eur. Phys. J. E: Soft Matter Biol. Phys.* **2003**, *12* (1), 101−110.
(62) Thickett, S. C.; Harris, A.; Neto, C. Interplay Between Dewetting and Layer Inversion in Poly(4-vinylpyridine)/Polystyrene Bilayers. *Langmuir* **2010**, *26* (20), 15989−15999.
(63) Ghezzi, M.; Thickett, S. C.; Telford, A. M.; Easton, C. D.; Meagher, L.; Neto, C. Protein Micropatterns by PEG Grafting on Dewetted PLGA Films. *Langmuir* **2014**, *30* (39), 11714−11722.
(64) Fetzer, R.; Jacobs, K. Slippage of Newtonian Liquids: Influence on the Dynamics of Dewetting Thin Films. *Langmuir* **2007**, *23* (23), 11617−11622.
(65) Fetzer, R.; Jacobs, K.; uuml; nch, A.; Wagner, B.; Witelski, T. P. New Slip Regimes and the Shape of Dewetting Thin Liquid Films. *Phys. Rev. Lett.* **2005**, *95* (12), 127801.
(66) Beysens, D. Dew Nucleation and Growth. *C. R. Phys.* **2006**, *7* (9−10), 1082−1100.
(67) Volmer, M.; Weber, A. Nucleus Formation in Supersaturated Systems. *Z. Phys. Chem.* **1926**, *119*, 277−301.
(68) Rose, J. W. Dropwise Condensation Theory and Experiment: A Review. *Proc. Inst. Mech. Eng., Part A* **2002**, *216* (2), 115−128.
(69) Furmidge, C. G. L. Studies at Phase Interfaces. I. The Sliding of Liquid Drops on Solid Surfaces and a Theory for Spray Retention. *J. Colloid Sci.* **1962**, *17* (4), 309−324.

DOI: 10.1021/acsami.5b06856
ACS Appl. Mater. Interfaces 2015, 7, 21562−21570